SLAC-PUB-629
November 1969
(EXPI)

ELECTRON AND PHOTON BEAMS AT NAL*†

W. T. Toner
Stanford Linear Accelerator Center
Stanford University, Stanford, California 94305

I. INTRODUCTION

Heusch[1] and Selove[2] have surveyed methods to produce electron and photon beams at a 200 GeV accelerator. From their work it is apparent that a neutral beam coming directly from the production target will have many orders of magnitude too many neutrons to be useful for photon physics. In this note we show that an electron beam chosen to give maximum flux will also have low hadron contamination. We point out that any high energy, high flux, pion beam can readily be converted into an electron beam. A 100 GeV electron beam with a pion contamination of $\sim 2 \times 10^{-4}$ will have about 1% of the flux of the same beam transport system when used as a pion beam.

II. BASIC BEAM

What seems the most promising method to make electron and photon beams is illustrated in Fig. 1. The extracted proton beam interacts in a light element (Be) target, followed by a sweeping magnet to remove charged particle background. Photons from π^0 decay convert to e^+e^- pairs in a radiator, R1. The optimum thickness of this radiator will most likely be about 0.3 radiation lengths. There follows a standard beam transport system focused on the EPB target, from which

---

*Work supported by the U. S. Atomic Energy Commission.

†This is a revised version of the report which appears in NAL 1968 Summer Study, Vol. 2, p. 125.

the e^+e^- pairs appear to originate. At the end of the beam the electrons may be used directly (in which case a gas threshold counter is probably necessary) or to produce a photon beam in a second radiator. The photon beam may be "tagged" at this point.

III. ADVANTAGES OF THIS METHOD

The electrons produced in R1 make such small angles with the direction of the photons producing them that they appear to come directly from the EPB target. There is only a small amount of broadening of this virtual source, due to multiple Coulomb scattering in R1.

This has the consequence that converting the π^0 decay photons outside the EPB target, rather than in it, does not dilute the density of electrons in phase-space. Therefore, using a thick, high Z, target in the first place and taking electrons directly from it would not result in any flux increase. And, of course, the pion background in a charged beam looking at the EPB target would be very severe.

In a 0.3 radiation length radiator (high Z), about one to two percent of the neutral (n, K^0, etc.) background will interact to produce secondary charged pions. These pions are produced at relatively large angles to the direction of the incident particle, and will appear to come from a diffuse region around the target. Coulomb scattering in .15 radiation lengths imparts an RMS transverse momentum of 8 MeV/c to the electrons, whereas the mean transverse momentum of the pions produced in R1 will be of the order of 300 to 400 MeV/c. If R1 is placed so that the apparent source due to multiple Coulomb scattering is slightly bigger than real target, the radius of the diffuse source of the pions will be 40 to 50 times bigger than that of the apparent source of electrons. The pion contamination, small to begin with, can therefore be reduced by a factor of about two thousand by collimation at a double, dispersion-free, focus of the beam.

Finally, we note that the design of the beam transport system for the electrons is in all ways identical with normal charged particle beam design. In fact, any hadron beam can easily be converted to an electron or photon beam by the addition of a sweeping magnet and radiator upstream of the first beam element. The sweep magnet should be oriented to bend vertically. If the dispersion-free second focus of such a beam is to be used to collimate out the pion halo, a final focusing stage will be needed, to clean up the background produced at the collimator.

IV. ELECTRON (POSITRON) FLUXES, RADIATOR THICKNESS

As pointed out by Heusch,[1] the electron flux from a thin radiator is related to the π^0 flux by the expression

$$N(E_\pm)\,dt\;\;dE_\pm = dt\;dE_\pm \int_{k=E_\pm}^{E\max} \frac{1}{k}\left[2\int_{E_{\pi0}=k}^{E\max} \frac{N_{\pi0}(E_{\pi0})}{E_{\pi0}}\;dE_{\pi0}\right] dk, \text{ --- } (1)$$

where dt is the (thin) radiator thickness in radiation lengths, $N(E_\pm)$ is the electron flux per steradian, GeV, radiation length and $N_{\pi0}(E_{\pi0})$ is the π^0 flux per steradian, GeV. The π^0 decay opening angle is neglected. Since the transverse momentum to the photon in the decay is less than 70 MeV/c, compared with ~350 MeV/c in the production process, the photon angular distribution will be very similar to the π^0 angular distribution at high energies.

The π^0 flux will be $N_{\pi0} = \frac{N_{\pi+} + N_{\pi-}}{2}$. This has been calculated from the 0° Hagedorn and Ranft spectrum[3] and is shown in Fig. 2. In order to get an idea of what is going on, we have used the approximation

$$N_{\pi0}(E_{\pi0}) \sim A(E_0 - E_{\pi0}) \text{ per GeV per steradian} \qquad (2)$$

Values of $A = .157$ per steradian per GeV^2 and $E_0 = 150$ GeV give curve (a) of Fig. 2. The approximation is excellent between 40 and 140 GeV.

The photon flux resulting is shown as curve (b) in Fig. 2. The dashed line includes the contribution from the π^o flux not accounted for by Eq. (2). Putting (2) into (1) and carrying out the integrations with E_0 as an upper limit, we get

$$\frac{N(E_\pm)\,dt}{2AE_0} = \left[1 - \frac{E_\pm}{E_0} - \log\frac{E_0}{E_\pm}\left(1 - 0.5\log\frac{E_0}{E_\pm}\right)\right] dt \tag{3}$$

Curve (c) of Fig. 2 shows the result, with $t = 0.2$ radiation lengths. The dashed line is a rough estimate of the effect of including the π^o not accounted for by Eq. (2).

For thick radiator we must write[4]

$$N(E_1)\,dE_1 = dE_1 \int_{t=0}^{T} \int_{E_\pm = E_1}^{E\max} \frac{N(E_\pm)}{E_\pm} \, \frac{\left(\log\frac{E_\pm}{E_1}\right)^{\left[\frac{4}{3}(T-t) - 1\right]}}{\Gamma\left(\frac{4}{3}(T-t)\right)} \, dE_\pm \, dt \tag{4}$$

with $N(E_\pm)$ given by the thin radiator expression of Eq. (1). Consider the fate of electrons produced in dt at $T-t = 0.75$. Equation (4) then simplifies to

$$N(E_1)\,dE_1 = dE_1\,dt \int_{E_1}^{E\max} \frac{N(E_\pm)}{E_\pm}\,dE_\pm \tag{5}$$

We may get a rough idea of the effect of this degradation in energy if we approximate the thin radiator yield $N(E_\pm)$ by a power law

$$N(E_\pm) \sim B\,E_\pm^{-n} \tag{6}$$

choosing the constants to fit Fig. 2 (c) at the energy E_1. This will give an over estimate of the flux above E_1. Putting (6) into (5) we have

$$N(E_1)\,dE_1 \leq dt\,dE_1\,\frac{B}{n}\left[E_1^{-n} - E_{\max}^{-n}\right] \tag{7}$$

A typical value of n is ~7 at 100 GeV. Thus the first part of a thick radiator will contribute less than 1/7 of the thin radiator flux, at the expense of using up some of the photon flux, and generating more pion background. It is clear that flux considerations alone will lead us to a thin radiator.

I would guess that a 0.3 radiation length radiator is probably close to the optimum, but this should clearly be worked out in more detail at the appropriate time. Along with this guess, goes another: that the appropriate value to use for t in this case is not 0.3 but 0.2, to allow for some loss by straggling. This is what was done to get Fig. 2 (c).

The steepness of this spectrum compared with the E^{-1} shape of the bremsstrahlung from the second radiator makes it obvious that 70 GeV photon physics will be better done using the bremsstrahlung of 75 GeV electrons rather than of 125 GeV electrons.

Table I shows some flux estimates for a typical 1μ sterad, 1% $\delta p/p$ beam.

V. HADRON CONTAMINATION

Neutral particles interact in R1 to produce hadrons. For an e^- beam we need only consider negative pions produced by incident neutrons.

The total flux of neutrons through R1 with energies greater than 125 GeV is roughly

$$50/\text{ster.}/\text{GeV}/\text{ interacting proton} \times 75 \text{ GeV} \times 10^{-6} \text{ ster.}$$

$= 3.8\ 10^{-3}$ per interacting proton. About $\frac{0.3 \times 5.8}{120} = 1.4\ 10^{-2}$

of them will interact. Assume (pessimistically) that the pion flux per interacting neutron is the same as the pion flux per interacting 200 GeV proton. Therefore $\frac{\text{pions produced in R1}}{\text{pions produced in primary target}} \sim 5 \times 10^{-5}$. We assume that we can get the factor of 2000 rejection discussed in paragraph 3, so that we have about $2.5\ 10^{-8}$ pions in the beam per pion of the same energy produced in the primary target.

Our 10^{-6} steradian beam accepts between 1% and 10% of the photon angular distribution, and the electron yield is roughly 1% of the pion yield (Table I). We therefore have $\frac{\text{pions in beam}}{\text{electrons in beam}} \sim 2.5\ 10^{-4}$.

These estimates are extremely crude, but they should be conservative. A photon beam derived from the electron beam in a thin radiator should be pure enough to use even without tagging. A relatively simple Cerenkov counter in the beam would allow it to be used for electron experiments.

VI. VERY PURE ELECTRON BEAMS

A method which might be considered for improving the purity of the electron beam is the reverse of the technique described by Barna et al.,[5] to remove electron contamination from a pion beam. It is to place a thin radiator at the first momentum analysis slit of the beam. Electrons which have radiated an amount of energy greater than the momentum resolution of the optical system may be separated from the other charged particles at the second, dispersion-free focus.

The momentum bite may be as factor of 10 more than the resolution. The radiated photon spectrum is $\sim \frac{tdk}{k}$. Consider a resolution of 0.1% and let us accept in the final stages of the beam an electron momentum bite of 10%. There will be t log 100 electrons which have radiated between 0.1% and 10% of their initial energy. For $t = .02$ this is about 9% of the electrons incident. (If we use $t \gtrsim .02$, we will have to use the correct straggling formula.)

VII. CONCLUSIONS

The best method to produce an electron beam at NAL is the one sketched in Fig. 1. The beam transport system might be any small angle, high energy hadron beam focused on the EPB target. The radiator should be thin (~ 0.3

radiation lengths), and placed as close to the first element in the beam as possible, consistent with a Coulomb scattering broadening of the apparent target of ~ the target diameter. The number of electrons in the beam per π^0 of the same energy produced in the EPB target is 1/27 at 75 GeV, 1/80 at 100 GeV and 1/250 at 125 GeV. This leads to electron fluxes per pulse of nearly 10^7 at 75 GeV down to a few times 10^5 at 125 GeV in 1% $\delta p/p$, 1μ ster. beam. Beam purity should be better than 2.5×10^{-4} π per electron.

Table 1

Energy	Initial π^0	γ incident on R1	Electrons
75 GeV	1.8 10^8	1.4 10^8	6.6 10^6
100 GeV	1.6 10^8	6.8 10^7	2.0 10^6
125 GeV	.96 10^8	2.2 10^6	.4 10^6

All fluxes are for 2×10^{13} protons interacting and for a solid angle of 10^{-6} ster. with a $\delta p/p$ of 1%.

REFERENCES

1. C. A. Heusch, UCRL-16830 III, 156 (1966);

   R. Wilson (private communication).

2. W. Selove, UCRL-16830 III, 151 (1966).

3. T. G. Walker, NAL Summer Study 2, 59 (1969).

4. Y. S. Tsai and V. Whitis, Phys. Rev. 149, 1248-1257 (1966).

5. A. Barna *et al.*, Phys. Rev. Letters 18, 360 (1968).

FIGURE CAPTIONS

1. Schematic diagram of electron/photon beam.
2. (a), (b) π^o and γ fluxes at 0^o per interacting 200 GeV proton.

   (c) Electron flux obtainable by converting the photons in a 0.3 radiation length radiator.

   The full curves are the result of approximating the π^o by $.157\ (E_\pi - 150)$. The dashed curves are estimates of the contribution from π^o not accounted for by the approximation.

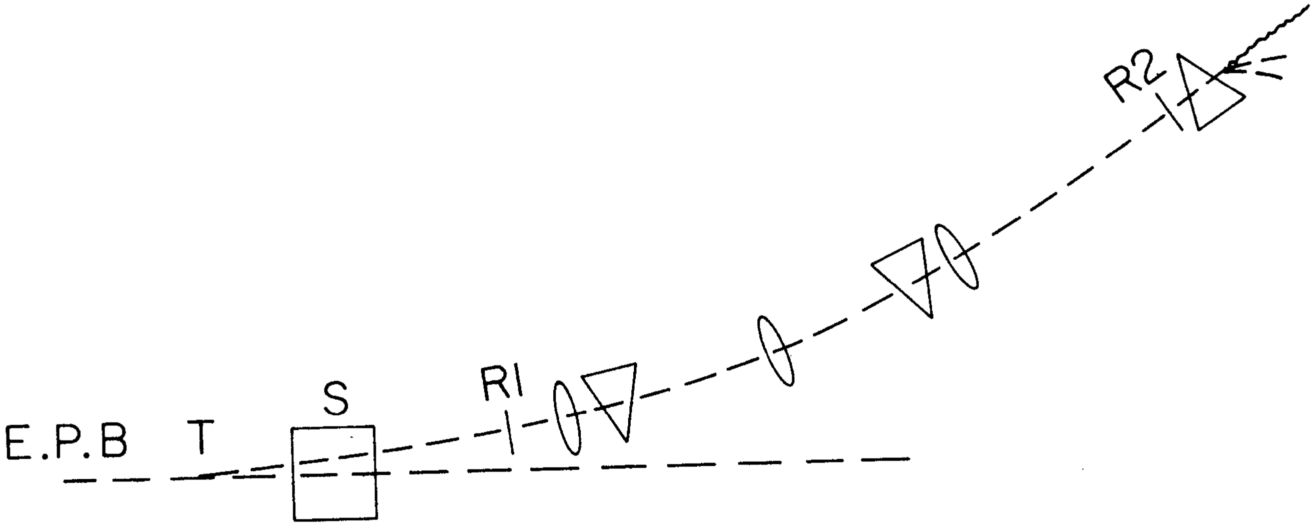

E.P.B: EXTRACTED PROTON BEAM
T: Be TARGET
S: SWEEP MAGNET BENDS IN VERTICAL PLANE
R1: RADIATOR $\gamma \rightarrow e^+ e^-$
R2: RADIATOR $e^\pm \rightarrow \gamma$

1386B2

Fig. 1

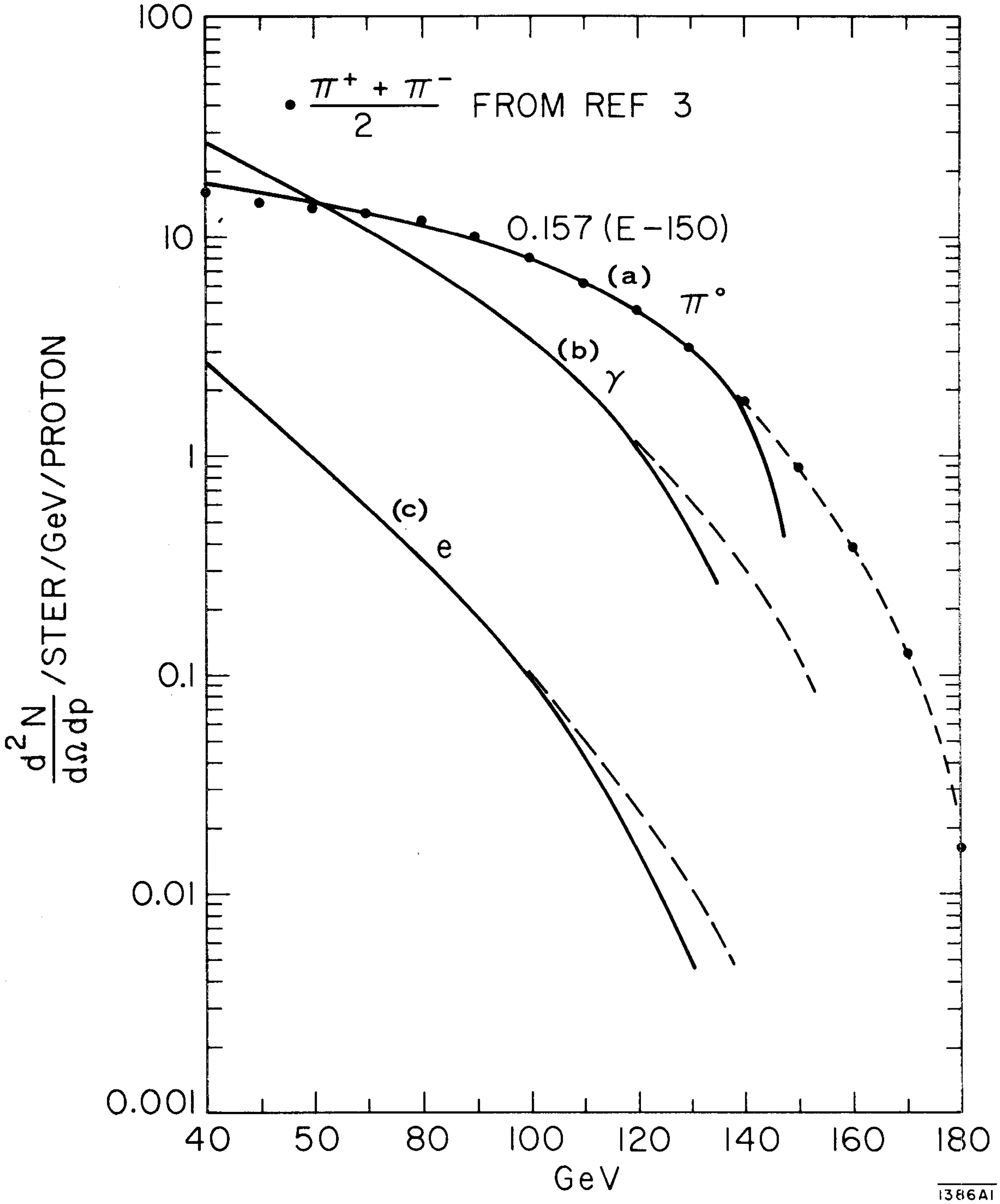

● $\frac{\pi^+ + \pi^-}{2}$ FROM REF 3
0.157 (E-150)
(a) π°
(b) γ
(c) e
100
10
1
0.1
0.01
0.001
40
50
80
100
120
140
160
180
GeV
$\frac{d^2N}{d\Omega dp}$/STER/GeV/PROTON
1386A1

Fig. 2